Predicting Surface Fuel Models and Fuel Metrics Using Lidar and CIR Imagery in a Dense, Mountainous Forest

Marek K. Jakubowski, Qinghua Guo, Brandon Collins, Scott Stephens, and Maggi Kelly

Abstract

We compared the ability of several classification and regression algorithms to predict forest stand structure metrics and standard surface fuel models. Our study area spans a dense, topographically complex Sierra Nevada mixed-conifer forest. We used clustering, regression trees, and support vector machine algorithms to analyze high density (average 9 pulses/m²), discrete return, small-footprint lidar data, along with multispectral imagery. Stand structure metric predictions generally decreased with increased canopy penetration. For example, from the top of canopy, we predicted canopy height (r² = 0.87), canopy cover (r² = 0.83), basal area (r² = 0.82), shrub cover (r² = 0.62), shrub height (r² = 0.59), combined fuel loads (r² = 0.48), and fuel bed depth (r² = 0.35). While the general fuel types were predicted accurately, specific surface fuel model predictions were poor (76 percent and <50 percent correct classification, respectively) using all algorithms. These fuel components are critical inputs for wildfire behavior modeling, which ultimately support forest management decisions. This comprehensive examination of the relative utility of lidar and optical imagery will be useful for forest science and management.

Introduction

Background

Fire is an important component of forest ecosystems in the Sierra Nevada, and was prevalent before widespread settlement in California (Skinner and Chang, 1996; Stephens and Collins, 2004; Sugihara *et al.*, 2006; Stephens *et al.*, 2007; Collins *et al.*, 2008). Many common Sierran plants exhibit fire-adapted traits such as thick bark and fire-stimulated flowering, sprouting, seed release, and germination (Sugihara *et al.*, 2006). In the last century, however, fuel loads in many Sierra Nevada forests have increased, likely as a result of fire suppression policies, warmer and moister climatic

Marek K. Jakubowski and Scott Stephens with the Department of Environmental Sciences, Policy and Management, University of California - Berkeley, 130 Mulford Hall, No. 3114. Berkeley, CA 94720 (marek@berkeley.edu).

Qinghua Guo is with the Department of Environmental Engineering, University of California - Merced.

Brandon Collins is with the USDA Forest Service, PSW Research Station, 1731 Research Park Drive, Davis, CA 95618.

Maggi Kelly is with the Geospatial Innovation Facility and Department of Environmental Sciences, Policy and Management, University of California - Berkeley, 130 Mulford Hall, No. 3114, Berkeley, CA 94720.

conditions, and the effects of past harvesting (Stephens and Ruth, 2005; Collins *et al.*, 2011a), putting the forests at risk of catastrophic fire (van Wagtendonk *et al.*, 1998; Miller *et al.*, 2009). In response to this risk, the US Forest Service is employing an approach that involves placing discrete fuel reduction treatments strategically across landscapes such that fire intensity is reduced not only within treated areas, but throughout the entire landscape (Finney, 2001; Moghaddas *et al.*, 2010).

In the US, modeling wildfire behavior and associated planning of fuel reduction treatments across landscapes are typically performed using FARSITE (Finney, 1998) and FlamMap (Finney, 2006). Both models rely heavily on Rothermel's fire spread model developed at the US Forest Service Fire Sciences Laboratory in Missoula, Montana (Rothermel, 1972). FARSITE and FlamMap require a standard suite of spatial data layers in order to run. These data layers include topography (elevation, slope, and aspect), forest structure (canopy cover, canopy height, crown base height, and crown bulk density), and surface fuel characterizations (referred to as "fuel models"). These data layers, co-registered and resolved at the same spatial resolution, are a fundamental input of most fire behavior models.

While all of these inputs influence the fire behavior models, surface fuel models are particularly important in determining fire behavior, as the Rothermel fire spread model predicts behavior of surface fire only. These fuel models (FM) consist of a set of surface fuel characteristics that describe stands based on dominant fire carrying fuel types (grass, shrub, tree litter, etc.) that include: fuel loads by fuel particle size class, fuel bed depth, surface-area-to-volume ratios for fuel particles, heat content, and dead fuel extinction moisture. This work proceeds under the assumption that surface fuel loads are related to forest composition and structure. Although this relationship has not been comprehensively studied, recent work in the Sierra Nevada has demonstrated robust relationships between fuel deposition rates and forest type/structure (van Wagtendonk and Moore, 2010). Surface FMs are divided into broad fuel types (e.g., shrub (SH), timber-understory (TU), and timber-litter (TL)), and then further into specific FMs: (e.g., "low load compact conifer litter" (TU1 181)). Thirteen models were first described by Anderson (1982) in a technical report, and more recently this list was expanded to 40 models (Scott and Burgan, 2005). In this paper, the updated 40-model set

was utilized since these models best describe the landscape in the study area.

In practice, a forest stand is assigned to one of these discrete surface FMs through a combination of field data, expert knowledge, and some type of either imagery interpretation or more automated remote sensing analysis (Collins et al., 2010). The field data includes plot-based descriptions of vegetation (height, diameter at breast height (DBH), species, density of trees and shrubs, and percent canopy cover), fuel load (the amount of litter, fuel bed depth, and fuel load noted as 1-, 10-, and 100-hour fuels), photographs, and a general description of the area (Keane et al., 1998; Bertolette and Spotskey, 1999). Expert knowledge typically involves iteratively selecting FMs such that predicted fire behavior is consistent with first-hand experience of fire behavior in actual fires (Collins et al., 2011b). Imagery is generally used to aid in FM selection across larger planning areas. While there is guidance aiding users in FM selection (Anderson 1982, Scott and Burgan 2005), the process of assigning FMs can be fairly subjective due to the common practice of incorporating expert opinion based on observed fire behavior. As a result, assignment errors can be introduced when FM descriptions are adjusted in order to produce fire behavior predictions more consistent with observed fire behavior (Varner and Keyes, 2009). This subjectivity can create inconsistency in FM assignments between users, resulting in substantial differences in predicted fire behavior (Varner and Keyes, 2009; Cruz and Alexander, 2010).

Wildfire Behavior Models and Remote Sensing
In typical circumstances where forest managers are faced with assessing fire behavior on a large scale, the cost, time, and technical challenges required to collect field data and to assign FMs make complete coverage of a forest is prohibitive. This is particularly true in areas with steep topography or in areas with limited access. In part to address these challenges, some recent efforts have experimented with more automated approaches using multispectral imagery (Riaño et al., 2002; van Wagtendonk and Root, 2003), hyperspectral imagery (Jia et al., 2006), or a combination of remotely sensed imagery and topography, climate, and disturbance data (Moghaddas et al., 2010). Yet, when FMs are estimated using remote sensing imagery, accuracy can be limited by the inability of sensors to capture the three-dimensional structure of the forest, especially when the tree density or stand height is high. Although hyperspectral image analysis offers more potential for species differentiation than multispectral data (Jia et al., 2006), neither of these passive remote sensing methods can accurately map 3D forest structure. Lidar presents advantages in this context as it is capable of describing the vertical structure of a forest stand and has successfully been used to map detailed forest parameters.

Previous Research
Lidar data is increasingly used to characterize forests across scales with direct measurements such as tree height, and derived measures such as biomass or leaf area index (LAI) (Wulder et al., 2008). At the stand scale, lidar has been used for canopy structure information (Lim et al., 2003). For example, Hollaus et al. (2006) correlated mean tree stand height, Hyyppä et al. (2001) extracted stem volume, Hudak et al. (2008) concentrated on the basal area and tree density, while Naesset and Gobakken (2008) and Popescu et al. (2003) extracted biomass. At finer scales, a number of studies have focused on extracting forest parameters from lidar at the individual tree level. For example, Lin et al. (2011) delineated individual trees in a mountainous forest from small-footprint lidar. Chen et al. (2006) and Koch et al.

(2006) tested a variety of watershed segmentation approaches to detect individual trees, while Persson et al. (2002) and Popescu et al. (2004) detected individual trees and correlated their measured height and/or crown diameter, respectively. Kaartinen et al. (2012) provide a good review of tree detection methods. Individual tree detection algorithms have typically been able to capture between 70 and 80 percent of individual trees (e.g., Persson et al., 2002; Kaartinen et al., 2012).

More recent lidar studies (often combined with optical imagery) focus on extracting fuel metrics across forest landscapes. Here, we refer to fuel metrics as continuous variables that contribute to the amount of overall fuel present at a site (both canopy and surface fuels): canopy height, canopy cover, crown base height (CBH), crown bulk density (CBD), total basal area (BA), shrub height, shrub cover, fuel bed depth, and fuel loads that compose of litter, 1-, 10-, and 100-hour fuel loads. The vast majority of this work focuses on extracting metrics that can be used in the previously mentioned fire behavior models, FARSITE and FlamMap. One of the first examples of a complete protocol for using lidar data in a fire modeling context is provided by Riaño et al. (2003). Andersen et al. (2005) used lidar to predict crown fuel weight, CBD, CBH, and canopy height of a western hemlock forest in Washington State at or above $r^2 = 0.77$. More recently, Erdody and Moskal (2010) used combination of lidar and color infrared (CIR) imagery to predict estimates of canopy fuel metrics in a mixed-conifer forest in Washington State. This study correlated height ($r^2 = 0.94$), CBH ($r^2 = 0.78$), CBD ($r^2 = 0.83$), and available canopy fuel ($r^2 = 0.89$) using lidar data alone. Although they did not test for statistical significance, all correlation coefficients were higher when imagery was added to the analyses. Similarly, Peterson (2005) and Peterson et al. (2005) analyzed lidar data from Sierra Nevada forests to extract CBH ($r^2 = 0.59$) and CBD ($r^2 = 0.71$). Skowronski et al. (2007) computed metrics in the Pinelands of New Jersey using lidar data alone and reported much higher variability in biomass estimation than the previously mentioned studies. The prediction accuracies depended on the forest types; specifically, the accuracies in the lowlands (pine and hardwoods) ranged from $r^2 = 0.59$ to 0.74, while in the highlands (conifer and deciduous mix) they ranged from $r^2 = 0.11$ to 0.33. Mitchell et al. (2011) and Gatziolis (2011) detected shrub height ($r^2 = 0.86$) and forest cover type (75.6 percent accuracy) using lidar in a shrub and forest environments, respectively.

Despite this progress, there are few examples demonstrating the efficacy of using lidar to derive surface FMs. One recent case is provided by Mutlu et al. (2008), who predicted seven of the original Anderson (1982) FMs using a Gaussian Maximum Likelihood classifier based on fusion of discrete-return lidar (2.6 points/m^2) and QuickBird imagery. The study reported very high accuracy levels: 90 percent with fusion of lidar and imagery, and 70 percent with imagery alone. However, the tested environment (small study area on mostly flat ground at an average elevation of less than 200 meters above sea level) is not typical of the mountainous forests in the western US. The latter forests are characterized by dense mixed-conifer vegetation at high elevations across large, topographically-complex areas. Since these more complex forests face increasing fire risk, evaluating the potential role lidar can play in mapping fuel models is valuable.

This research evaluates the use of small footprint, discrete return lidar data (alone and fused with optical remotely sensed imagery) to extract canopy fuel information from dense mixed-conifer forests across complex topographical terrain. The objectives are to determine: (a) whether relationship exists between surface FMs derived from

measured field data and remotely sensed lidar, optical imagery, or combinations thereof, and (b) whether fuel metrics (both those that are directly used in the assignment of FMs, and those that directly feed fire behavior models) can be predicted reliably from lidar, optical imagery, or combinations of these data. The study domain in this research is larger than the previous studies of the same focus (e.g., Mutlu *et al.*, 2008; Erdody and Moskal, 2010) and uses higher density lidar pulse posting, resulting in a more complete representation of the forest. It is also part of a larger study, Sierra Nevada Adaptive Management Project (SNAMP), a multi-discipline collaborative effort among land managers, researchers, and interested stakeholders, designed to explore the effects of coordinated landscape fuel treatments (Collins *et al.*, 2011b).

Methods

We analyzed relationships among lidar, imagery, surface fuel models, and forest structural metrics in a classification and regression contexts. We used a range of classification methods to evaluate the relationship as well as the methods' relative performance. To predict FMs we used simple *k*-means classifier, two regression trees (random forest and classification and regression trees), and support vector machine (SVM) algorithms. To predict fuel metrics we used linear and additive regression models, and regression-based SVM. Based on preliminary results, we used all lidar returns in the analyses described below. The workflow is shown in Figure 1.

Study Area

Our study area is located in the northern part of the Sierra Nevada of California (centered at 39° 07′ N, 120° 36′ W) in Tahoe National Forest, about 35 km west of Lake Tahoe. It encompasses 99.5 km^2 of topographically complex and steep terrain with elevations ranging from 600 m to 2,186 m above sea level (Figure 2). The average precipitation since the record began in 1990 is 1,182 mm/year in this Mediterranean climate. Almost the entire study area is forested: only 7 percent of the area is non-conifer forest according to the Tahoe National Forest criteria (<10 percent of coniferous tree
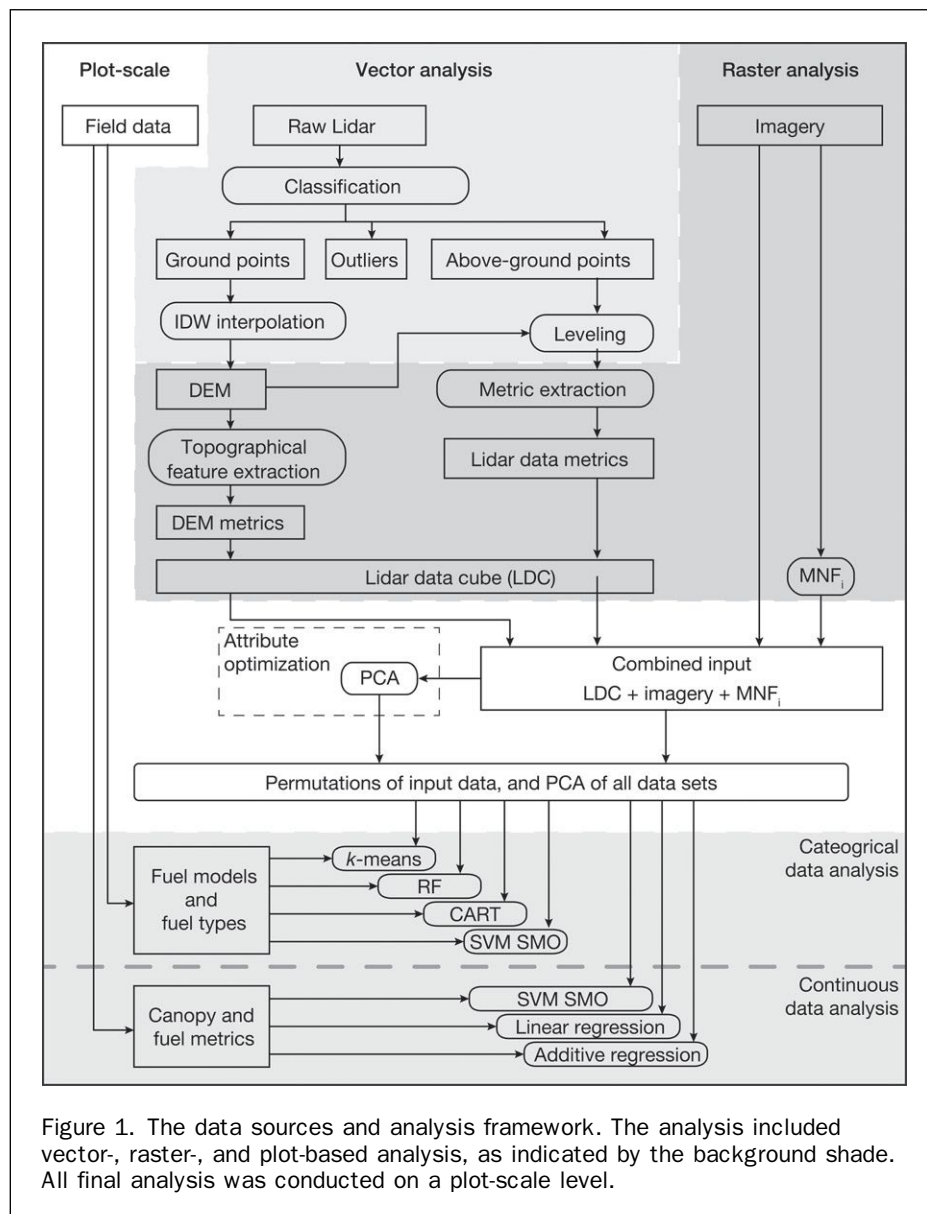

Figure 1. The data sources and analysis framework. The analysis included vector-, raster-, and plot-based analysis, as indicated by the background shade. All final analysis was conducted on a plot-scale level.
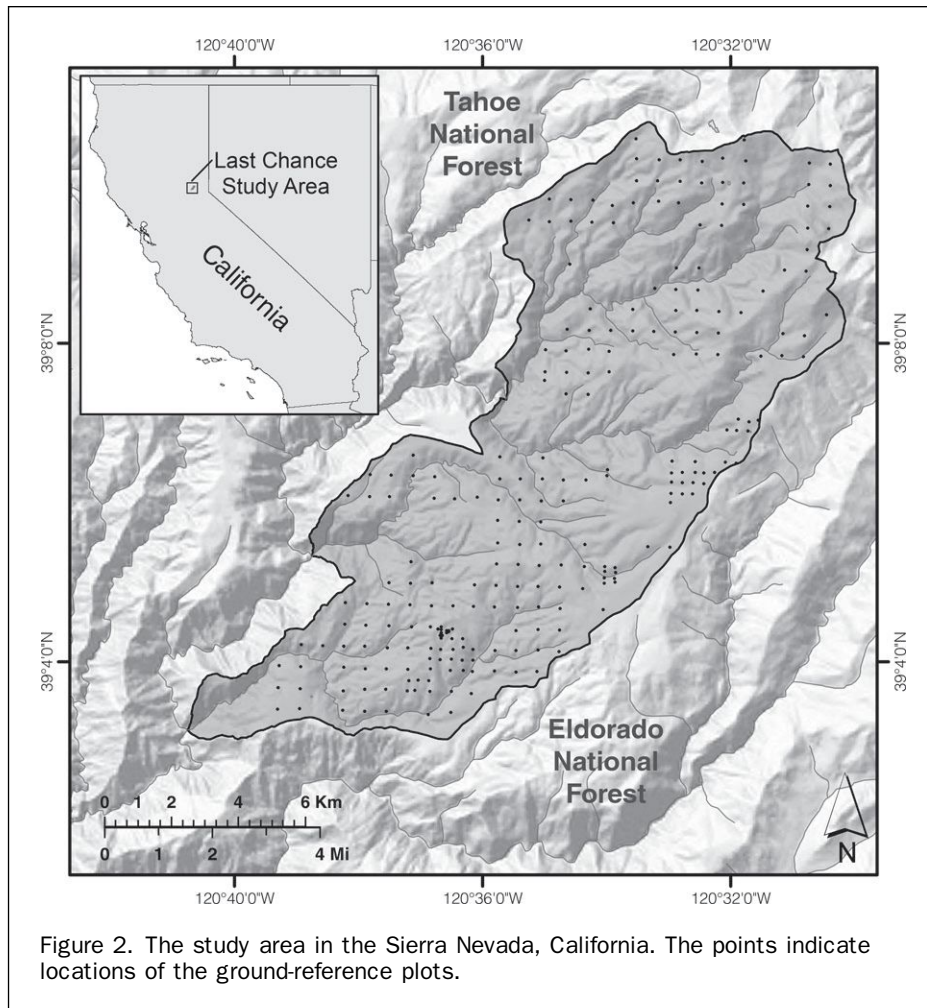
Figure 2. The study area in the Sierra Nevada, California. The points indicate locations of the ground-reference plots.

crown area). Fire scars recorded in tree rings from adjacent areas indicate low-severity fires with high-frequency occurrence from 5 to 15 year intervals (Stephens and Collins, 2004).

The dominant vegetation is dense mixed-conifer forest where dominate tree species include sugar pine (*Pinus lambertiana*), ponderosa pine (*P. ponderosa*), incense-cedar (*Calocedrus decurrens*), red and white firs (*Abies magnifica* and *A. concolor*), as well as California black oak (*Quercus kelloggii*). The study area is under management of the US Forest Service, with a few private in-holdings scattered throughout.

Data
Field Data
Field data characterizing a range of forest parameters was collected at 248 circular plots covering the study area. The plot centers were distributed across UTM grid with 500 m spacing at even coordinate junctions. The plot centers were offset by 25 m in random direction when the desired coordinates fell on road surfaces, landings, rivers, or otherwise physically inaccessible locations. The field data was collected over the course of two summer field seasons in 2008 and 2009; in total, 2,340 trees were measured. The plots were extensively mapped for validation of lidar data. Each plot covers a 500 m^2 area with a 12.62 m radius. All trees above 19.4 cm DBH were tagged with a unique numerical ID. Tree height, DBH, height to live crown base (HTLCB), species, and crown class were recorded along with

the unique ID. HTLCB is defined in this study as the lowest extent of vertically continuous live crown on an individual tree. In instances where the crowns of smaller trees are touching the crowns of larger trees the HTLCB measurement includes the smaller tree. Trees with DBH between 5 and 19.5 cm were also measured using the above protocol, but no numerical IDs were assigned. We also sampled shrub cover and surface/ground fuels using three randomly chosen transects on each plot. The shrub information includes height, percent cover, and species. The fuel information includes tallies of fuel intersections with each transect by fuel particle size class (1-, 10-, 100-, and 1,000-hour time lag), as well as, litter, duff, and total fuel heights. For more information regarding fuel inventory methodologies see Brown and Roussopoulos (1974) and Collins *et al.* (2011b). Five digital photographs were also taken at each plot in four directions and towards the sky.

In addition to the measurements described above, we generated shapefiles with precise locations and IDs for all tagged trees. We used a combination of Trimble's GeoXH global positioning system (GPS) with an Impulse Laser Rangefinder and an Impulse Electronic Compass to create the stem map shapefiles. At first, two approximately perpendicular angles were used to obtain positions of all trees; however, our analysis throughout the field season indicated that two angles did not sufficiently improve the positional accuracy of the trees to justify their collection at each plot. The position of the trees were measured and recorded using a laser range-finder and electronic compass

combination, and georeferenced to a differential GPS position. The locations of large marker trees were recorded outside of the plot boundary to improve the positional accuracy with respect to lidar data. The individual trees were marked with steel markers, whereas the plot centers were established by rebar hammered into the ground (Figure 3). Each plot shapefile includes positions of all tagged trees and their ID, position of the GPS antenna, and the plot center. The tree positions were later adjusted to true tree centers based on the measured DBH (Figure 3). The tree structure data described above (height, species, etc.) were merged to each tree location based on the assigned ID number.

To georeference the stem map shapefiles, we positioned the GPS at most 30 m away from the plot center (typically within the plot or at the plot center) where there was relatively little canopy above to obtain a small positional dilution of precision (PDOP); we filtered the obtained GPS data to a maximum PDOP value of 5. For each GPS position, we collected at least 300 measurements, although the majority of positions included about 1,000 and up to 7,700 measurements recorded at a 1 second interval. We used a Trimble GeoXH differential GPS with Trimble Zephyr Antenna on top of a 3 m GPS antenna pole to minimize multipath problems. Continuously Operating Reference Stations (CORS) and University NAVSTAR Consortium (UNAVCO) stations less than 20 km away from all field measurements were used for differential GPS post-processing. Finally, large, easily identifiable "marker" trees up to 50 m from the plot center were measured and spatially located to increase the accuracy and matching between lidar and ground reference data.

Fuel Metrics
In this work, "fuel metrics" comprise the following continuous metrics: canopy height (maximum and mean), canopy cover, BA, CBH, CBD, shrub height, shrub cover, combined fuel load, 1,000-hour fuel load, and fuel bed depth. Using the information collected from fuel transects we calculated surface fuel loads for each plot. These calculations were based on the species-specific coefficients reported in Wagtendonk *et al.* (1996 and 1998), weighted by the proportion of BA of each species (Stephens, 2001). We summarized these fuel loads into three pools: (a) combined fuel load composed of litter and smaller woody fuels (1- to 100-hour fuel loads), (b) coarse woody fuels (1,000-hour), and (c) total fuel. In addition to surface fuel loads, we calculated two canopy fuel metrics at the stand scale: CBH and CBD. CBH is defined as the mean lowest height above the ground at which there is sufficient available canopy fuel to propagate fire vertically through the canopy (Scott and Reinhardt, 2001). CBD is the oven-dry mass of available canopy fuel per unit volume (Scott and Reinhardt, 2001). We calculated these using established allometric equations (Reinhardt *et al.*, 2006a; Reinhardt *et al.*, 2006b) using Fuels Management Analyst (Carlton, 2005) and the collected plot tree measurements.

Fuel Models
The field data described above were used to assign FMs. The FMs were assigned using a decision tree protocol adapted for our study area from Scott and Burgan (2005). The basic summary of the protocol is illustrated in Figure 4. In particular, fuel load, fuel depth, shrub coverage and height, tree composition, and general forest stand structural information were used to establish repeatable criteria for these metrics. The criteria were then used to systematically assign one of the 40 FMs to each plot. Two classes, "low load dry climate timber-grass-shrub (model TU1)" and "very high load, dry climate timber-shrub (model TU5)," had many more samples ($n = 77$ and $n = 33$, respectively), than the rest of the FM classes.
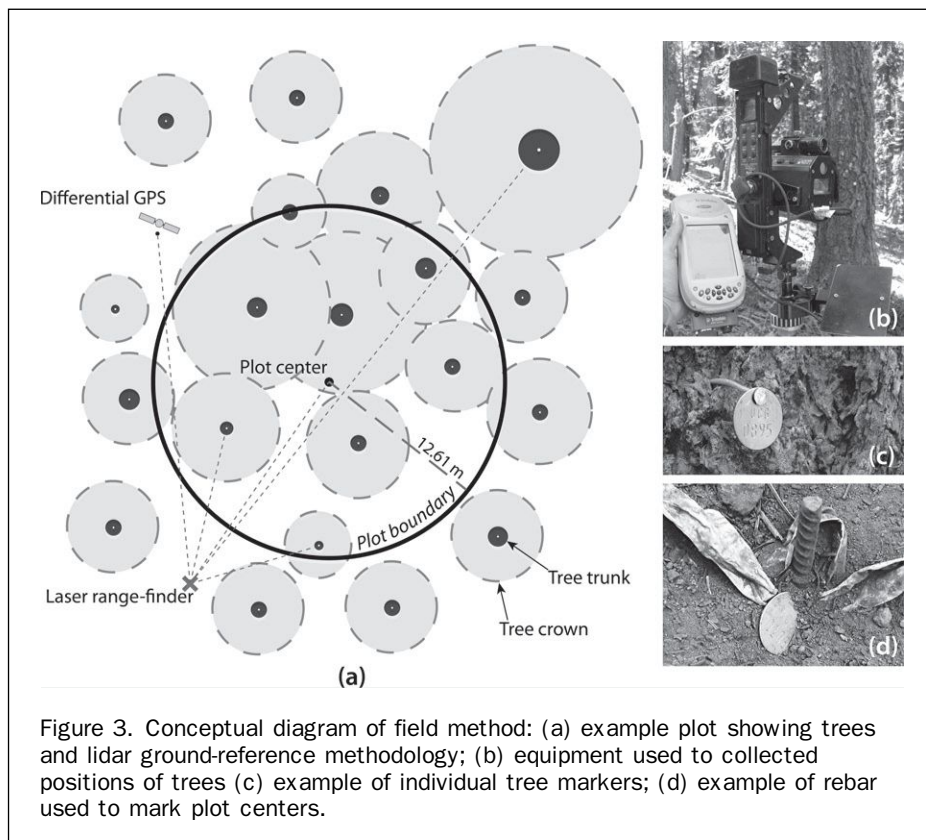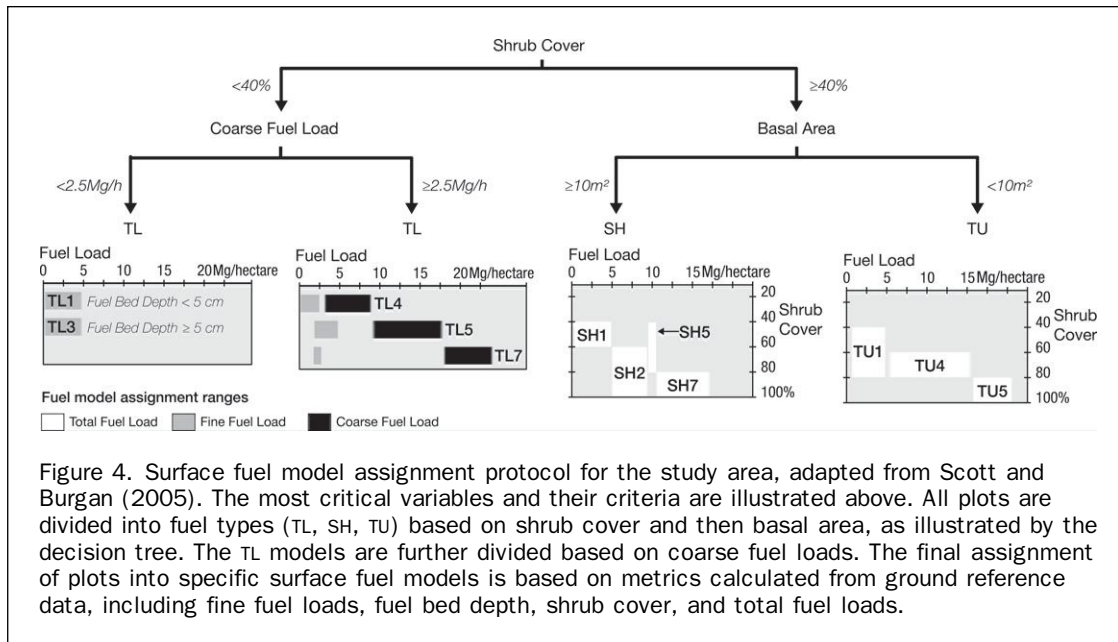

Figure 3. Conceptual diagram of field method: (a) example plot showing trees and lidar ground-reference methodology; (b) equipment used to collected positions of trees (c) example of individual tree markers; (d) example of rebar used to mark plot centers.

Figure 4. Surface fuel model assignment protocol for the study area, adapted from Scott and Burgan (2005). The most critical variables and their criteria are illustrated above. All plots are divided into fuel types (TL, SH, TU) based on shrub cover and then basal area, as illustrated by the decision tree. The TL models are further divided based on coarse fuel loads. The final assignment of plots into specific surface fuel models is based on metrics calculated from ground reference data, including fine fuel loads, fuel bed depth, shrub cover, and total fuel loads.
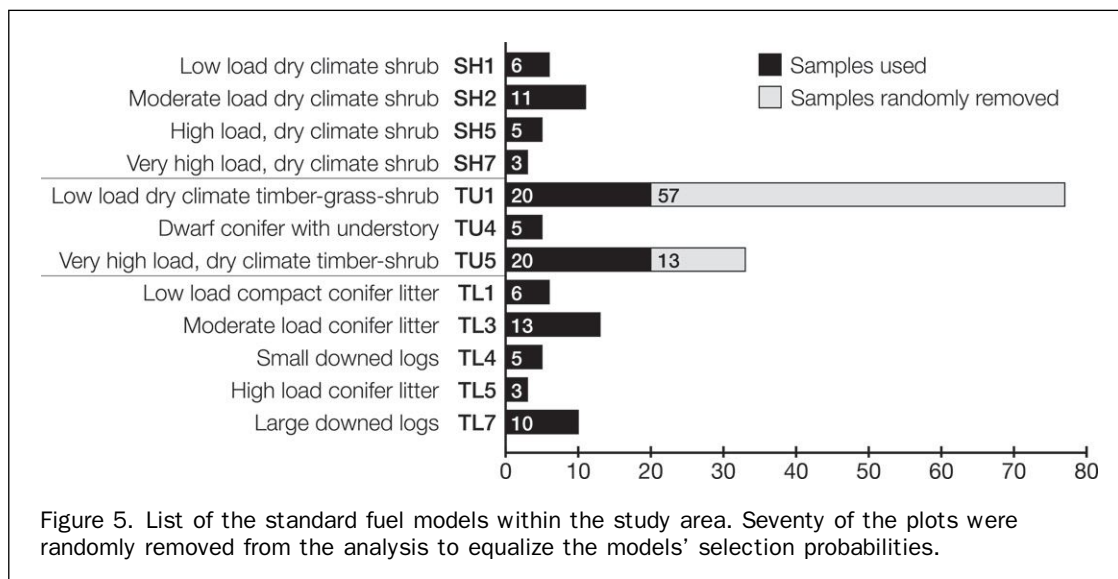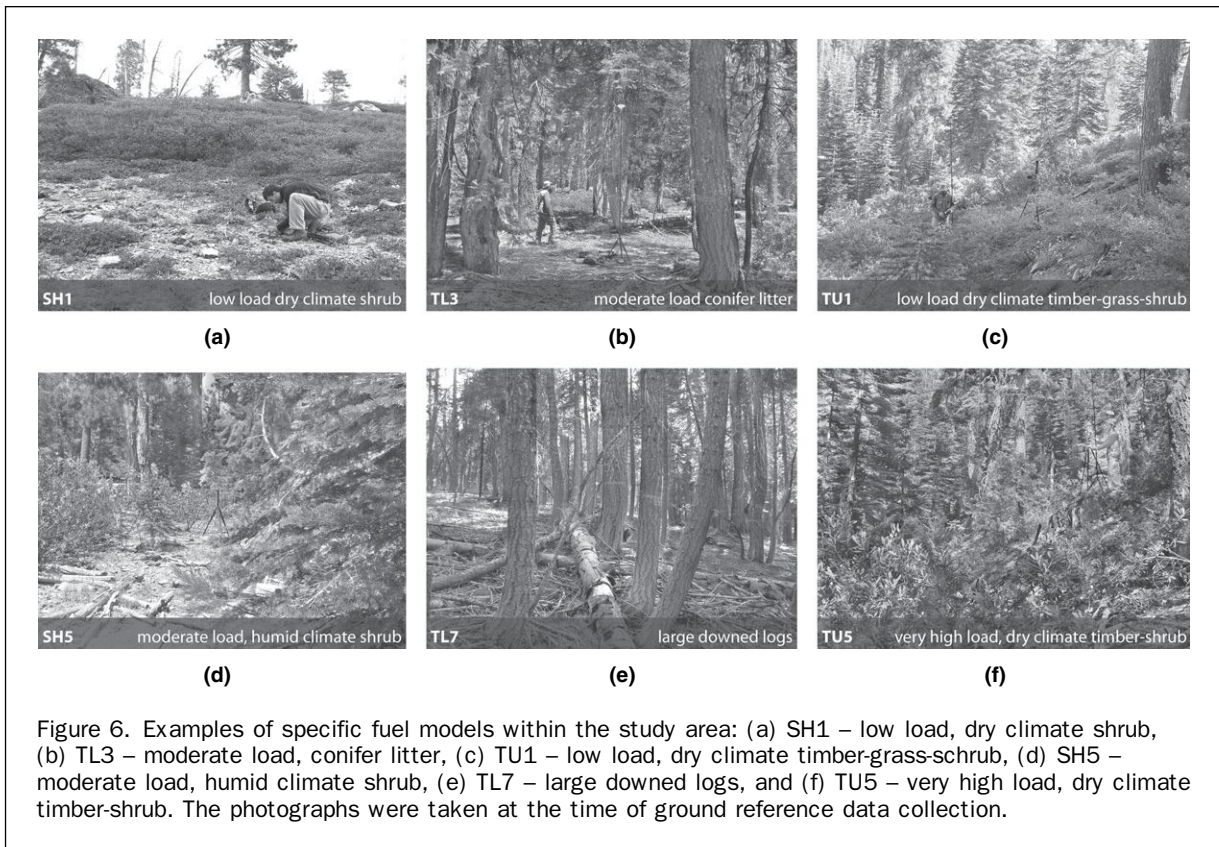
We randomly removed samples from these two FMs to equalize their selection probabilities with respect to the other classes and remove selection bias. In the end we used 12 FMs with N = 107 (Figure 5). Sample photographs taken at the time of ground reference data collection (Figure 6) depict a few FMs within the study area.

Lidar Data
Lidar data was collected by National Center for Airborne Laser Mapping (NCALM) using the Optech GEMINI Airborne Laser Terrain Mapper (ALTM) sensor at an altitude of approximately 1,000 m above ground level (AGL). The data was collected in five survey flights from 18 September to 21 September 2008 in leaf-on conditions. The relative horizontal and vertical accuracy were reported and had been independently confirmed to be approximately 5.5 to 10 cm and an average of 7.5 cm, respectively. Up to four returns

per each laser pulse were recorded along with 12-bit dynamic range intensity. Due to steep topography, the pulse rate frequency (PRF) was limited to 70 KHZ and the scan angle to ± 20 degrees. To increase point density, the aircraft flew twice over the area with a large overlap, such that every ground point was acquired from at least three (and mostly four) angles to yield an average of nine and minimum of six pulses/m^2. Since the lidar system records up to four returns per pulse, the total return density in heavy canopy was often greater than 20 points/m^2. We applied a buffer around the study area to ensure all parts were surveyed and consequently surveyed total area of 107 km^2. The data was delivered in Universal Transverse Mercator (UTM) coordinate system with respect to 1983 North American Datum (NAD83); orthometric heights were computed using NGS GEOID03 model in North American Vertical Datum of 1988.

Figure 5. List of the standard fuel models within the study area. Seventy of the plots were randomly removed from the analysis to equalize the models' selection probabilities.

Figure 6. Examples of specific fuel models within the study area: (a) SH1 – low load, dry climate shrub, (b) TL3 – moderate load, conifer litter, (c) TU1 – low load, dry climate timber-grass-schrub, (d) SH5 – moderate load, humid climate shrub, (e) TL7 – large downed logs, and (f) TU5 – very high load, dry climate timber-shrub. The photographs were taken at the time of ground reference data collection.

Lidar Preprocessing

The raw lidar data was processed by NCALM using Terra-Solid's TerraScan software (Soininen, 2012) to remove obvious outlier points, including isolated point removal (points with no neighbors within five meters) and "air point" removal, where points clearly above the canopy are compared to their neighbors. The point cloud was then classified to ground, above-ground, and outlier points using an iterative triangulated surface model. Our preliminary analyses indicated that the combination of ground and above-ground points leads to best results thus we used both classes in the analyses. A digital elevation model (DEM) was processed at 1 meter resolution using Inverse Distance Weighted (IDW) interpolation based on suggestions from past research (Guo *et al.*, 2010).

To ensure maximum accuracy, we extracted and only used lidar points within circular area above each plot (12.6 m radius). We developed a set of MATLAB functions to extract lidar metrics in a raster format at a user-defined, horizontal spatial resolution. The lidar metrics (Table 1) include descriptive metrics (e.g., *maximum height*, or *number of points from 0.5 to 1 m*) and statistically-based metrics (e.g., *0.05 percentile* and *standard deviation*). The metrics were calculated with respect to ground level. For example, *maximum height* describes the distance between the highest recorded lidar point within a moving window cell and the ground elevation as defined by the DEM. Similarly, *point density 0.5 to 1 m* is the number of lidar returns recorded between 0.5 m and 1.0 m normalized by the total number of returns within a raster cell above the DEM elevation. The plot rasters include a set of bands, each

TABLE 1. VARIABLES THAT CONTRIBUTED TO ANALYSES; THE METRICS THAT DIRECTLY SUMMARIZE LIDAR WERE DERIVED FROM PULSE RETURNS WITHIN THE FIELD PLOT FOOTPRINTS; ALL IMAGERY METRICS WERE CALCULATED ON A 20 METER SIZE GRID; THE LIDAR HEIGHTS ARE CALCULATED RELATIVE TO THE GROUND LEVEL, AS INDICATED BY THE LIDAR-DERIVED DEM.

Lidar Data Cube (LDC)

Elevation	Point density 0 to .5 m
Slope	Point density .5 to 1 m
Aspect	Point density 1 to 1.5 m
Height: minimum	Point density 1.5 to 2 m
Height: mean	Point density 2 to 3 m
Height: maximum	Point density 3 to 4 m
Height: standard dev.	Point density 4 to 5 m
Percentile 0.01	Point density 5 to 10 m
Percentile 0.05	Point density 10 to 15 m
Percentile 0.10	Point density 15 to 20 m
Percentile 0.25	Point density 20 to 25 m
Percentile 0.50	Point density 25 to 30 m
Percentile 0.75	Point density 30 to 35 m
Percentile 0.90	Point density 35 to 40 m
Percentile 0.95	Point density 40 to 45 m
Percentile 0.99	Point density 45 to 50 m
Total number of returns	Point density 50 to 55 m
	Point density 55 to 60 m

Imagery Variables

NAIP: blue band	MNF component 1
NAIP: green band	MNF component 2
NAIP: red band	MNF component 3
NAIP: NIR band	MNF component 4

band describing a different lidar data metric. In practice, the user may choose any pixel size to generate a wall-to-wall map, although in this case the pixel size was irrelevant since all lidar data above each plot were summarized into a single point. While there may be a slight difference between results based on a circular footprint and a square pixel, we believe that it would be insignificant.

We then extracted topographical information based on DEM derived from lidar data classified as ground points. All topographical measures (Table 1) were derived from the DEM using ITT's ENVI 4.7 Topographical Modeling feature (ITT Visual Information Solutions, 2009). This step was processed at 20 m resolution to be consistent with the remaining spatial and ground reference data. The plot raster data described above were combined with the topographical information into a raster dataset (lidar data cube, or the LDC) with a set of bands similar to a hyper-spectral image cube, where each band describes a different lidar or topography metric. The LDC was saved into a 32-bit, floating-point Tagged Image File Format (TIFF) raster format to increase compatibility with external analysis software. A TIFF Worldfile and an ENVI header file were generated to preserve metadata and description of each metric. The band data for all plots were then extracted to a table for analysis within data mining software, as described in the Analysis section.

Imagery
We augmented the LDC by adding four-band visible near-infrared (VNIR) multispectral imagery from the National Agricultural Imagery Program (NAIP). The 1 m ground sample distance (GSD) imagery was collected and orthorectified in 2009. In preliminary analysis we simply added the multispectral values or their Principal Component Analysis (PCA) and/or Minimum Noise Fraction (MNF) transforms at the pixel level; however, this did not affect the prediction rates of the dependent variables. As a result, we resampled the imagery to 20 m using simple averaging to keep all data resolutions consistent. Analysis of the eigenvalues indicated that using four MNF bands was appropriate.

Analysis
Input Data for All Analysis
We conducted all analyses using four combinations of the LDC, raw multispectral imagery, and MNF of the imagery (MNF$_i$) (Figure 1). Specifically, we used the following four combinations of the input data: (a) LDC, (b) LDC + multispectral imagery, (c) LDC + MNF$_i$, and (d) PCA of the combination of LDC and multispectral imagery. All further analyses were performed in Waikato Environment for Knowledge Analysis (WEKA), a set of data mining algorithms compiled into a software package at the University of Waikato, New Zealand (Frank *et al.*, 2010).

Feature Optimization
Preliminary analysis using the complete dataset yielded low prediction rates due to overfitting. Thus, we optimized each of the four data combinations by using the optimization routine suggested by WEKA and designed for the subsequent analysis. For example, for data input to random forest we optimized input data with filtered subset evaluator using greedy stepwise search method. In each of these processes, the overall dataset was narrowed to include the most influential input variables in the subsequent analysis. In addition, we ran a PCA on the LDC and imagery dataset and analyzed the six principal components based on the eigenvalues which explained 98.04 percent of the dataset variability.

Fuel Model Analysis
We used a number of classification algorithms to evaluate the performance of simple and complex models (e.g., clustering and SVM algorithms, respectively) in predicting FMs using the four combinations of input data. The training data was randomly selected from the input data using a ten-fold validation method. We used all the methods described below to classify specific surface FMs as described in Figure 5 (e.g., TU1, TU4, TU5, SH1, etc.), as well as generalized surface fuel model types (SH, TU, and TL).

First, we used a simple *k*-means classifier to cluster the input spatial data into FMs. The *k*-means algorithm distributes data into *k* classes by calculating the Euclidean distance between each data point and an estimated class mean in feature space. The means are then reassigned iteratively to minimize the distances among data points and the class means (Duda *et al.*, 2001). Next, we used two regression tree algorithms: random forest (RF) and SimpleCART. The RF algorithm uses an ensemble classifier (multiple models) to obtain better predictive performance. The classifier generates a large number of decision trees at random, a subset of which is chosen to construct the final model (Breiman, 2001). SimpleCART is WEKA's implementation of a classification and regression tree (CART) algorithm (Feldesman, 2002). CART is a nonparametric algorithm that divides a large number of input variables and their interactions based on goodness of split criteria. The process generates a large number of splitting decisions and then applies a set of rules to reduce them (i.e., to prune the tree). CART makes no assumptions about the statistical distribution of its independent or dependent variables, which also means that it cannot generate a probability level or confidence interval (Feldesman, 2002). One of the differences between CART and RF is that RF bootstraps the data to provide a more honest and conservative assessment.

Finally, we used the sequential minimal optimization (SMO) learning algorithm, a type of SVM. In general, SVM algorithms are based on statistical learning theory; they classify datasets by fitting a hyperplane in the feature space to only the data points closest to the class boundaries. These data points are the support vectors. SVM uses structural risk minimization, which minimizes the probability of misclassification based on probability distributions. By utilizing only the points closest to the boundary hyperplane, the SVMs are well suited for classification problems of high-dimensional datasets with a small training sample size (Hsu *et al.*, 2003). Most specifically, the SMO algorithm globally replaces all missing values and transforms categorical attributes into binary classes (Keerthi *et al.*, 2001).

Fuel Metric Analysis
We used simple multiple linear regression, additive regression, and SVM models to predict the fuel metrics. The additive regression model is an iterative process in which the residuals of a multiple linear regression model are used to construct a new model. All iteration predictions are added to calculate the final prediction model. We reduced the learning rate parameter to prevent overfitting the data (Friedman, 2002; Frank *et al.*, 2010). In this instance, we used WEKA's regression implementation of the SMO in combination with the parameter learning algorithm, RegSMOImproved (Keerthi *et al.*, 2001). We used ten-fold cross-validation as suggested by previous research (Kohavi, 1995) and the corrected paired t-test with two-tailed 0.05 confidence-level to verify all the results.

Results

Fuel Model Results

We analyzed lidar metrics and CIR imagery to predict the assigned surface FMs using four different classification algorithms. We report the results as the percentage of correctly predicted models based on a comparison to the field data because the dependent variable is categorical (Table 2). The best classification was obtained using a combination of lidar and MNF transform of the imagery with the CART algorithm; however, all specific surface FM results were poor (below 50 percent). The simple *k*-means classifier correctly predicted 24 percent of the FMs, based on the lidar data alone. The regression tree classifications algorithms, RF and SimpleCART, predicted between 31 percent and 45 percent of the FMs correctly, depending on the data input and the classifier. The CART algorithm most consistently outperformed the RF. The machine learning algorithm, SMO, correctly predicted between 21 percent and 38 percent, depending on the data input and the classifier. We used various data input combinations, including the LDC, imagery, combination of LDC and imagery, and their transforms; we found that with most methods, either lidar data alone or lidar data with MNF of the imagery performed best. The PCA of the entire dataset (LDC + imagery) performed poorly in nearly all cases.

We also classified the broader fuel types: SH, TU, and TL. These results (Table 2) improved, suggesting that while lidar may not be able to accurately predict specific surface FMs, it is capable of assessing fuel types. The best overall predictor was the SMO machine learning algorithm (76 percent correctly classified). The difference among various data inputs was small, ranging from 73 percent to 76 percent, and the simplest data input (lidar data alone) attributed to 75 percent correct classification. Although the regression trees predicted these classes relatively well (RF's best at 75 percent and CART's best at 72 percent correctly classified) no algorithm has predicted the fuel types as consistently and accurately as the SMO. We found that the results were not improved after feature optimization of the input data. Consequently, all input variables (within the LDC and derived from the imagery) were used.

Fuel Metric Results

We analyzed the same set of input data to predict 12 fuel metrics using linear- and additive-regression models, and

the SMO algorithm (Table 3). We split the metrics into two categories: those that are used to assign FMs (BA, shrub height, shrub cover, combination of 1-, 10-, and 100-hour fuel loads, and fuel bed depth) and those that directly feed fire behavior models such as FARSITE (canopy height, canopy cover, CBH, and CBD). The range in prediction rates is large across models and data inputs but there are trends (Table 4). The best prediction rates were associated with maximum canopy height (r^2: 0.69 to 0.87), BA (r^2: 0.67 to 0.82), and canopy cover (r^2: 0.62 to 0.83), followed by shrub cover (r^2: 0.40 to 0.62) and shrub height (r^2: 0.40 to 0.59). All other prediction rates (and all directly related to measures of fuel), were below $r^2 = 0.5$ (combined fuel loads, CBH, fuel bed depth, 1,000-hour fuel loads, and CBD, in decreasing order of prediction rates). All other individual fuel load categories (e.g., litter, 1-, 10-, 100-hour loads) yielded very poor correlation coefficients and are not reported here.

Table 4, arranged by best Pearson's correlation coefficient and the associated method, provides a simplified summary of all the fuel metric results. The SMO algorithm outperformed the other models in 5 out of the 11 cases using the PCA-transformed data. The SMO performed well mostly with metrics that are more difficult to assess using lidar and imagery: metrics that describe the understory and fuel loads. Multiple linear regression model worked best when predicting less complex metrics (canopy height and BA), in which case data transformations made little or no difference. The additive regression performed best only in cases where the results were poor (1,000-hour fuel loads and CBD). Although we performed feature optimization on all input data, we found that the results were not improved. Consequently, all input variables (within the LDC and derived from the imagery) were used.

Discussion

Our results of forest structural metrics are good, and in general meet or exceed those from previous studies. For example, Lefsky *et al.* (1999) reported r^2 of 0.49 when explaining BA with lidar data compared to our regression model which resulted in an r^2 of 0.82. Lefsky *et al.* (2002) analyzed waveform lidar to predict canopy cover and reported mean r^2 of 0.84, 0.63, and 0.11 from boreal coniferous, temperate coniferous, and temperate deciduous forests, respectively; however, when the entire dataset was considered, their estimates decreased to r^2 of 0.37 (as compared to $r^2 = 0.83$ in our work). Riaño *et al.* (2007) predicted shrub height using lidar at $r^2 = 0.48$ to 0.65, which is comparable to our work (shrub height $r^2 = 0.59$; shrub cover $r^2 = 0.62$).

In contrast, a few studies predicted CBD with higher accuracy, including Andersen *et al.* (2005), Erdody and Moskal (2010), and Saatchi *et al.* (2007) with r^2 of 0.86, 0.83, and 0.84, respectively. Similarly, Erdody and Moskal (2010), and Andersen *et al.* (2005) predict CBH and ln(CBH) with r^2 of 0.78 and 0.77, respectively. There are a few possible reasons for why the results in our study differ from these two studies. First, the forest composition and topography of our study area is more complex than the previously mentioned projects, which could affect the penetration of the laser. Second, the CBD metric is quite sensitive to modeling assumptions used to derive it, including the CBH and stand height (Andersen *et al.*, 2005), which may have contributed to the lower correlation coefficients in present work. Third, the Andersen *et al.* (2005) study did not measure crown base heights or tree heights for many trees in the field, and therefore the reported results may contain significant errors. Finally, Saatchi *et al.* (2007) summarized his findings based on a radar, not lidar, system. Thus, it would be worth

	Specific standard fuel models		
	Clustering	Regression Tree	Machine Learning
Data input	*k*-means	RF	CART	SMO
Lidar alone	24	35	35	**37**
Lidar + imagery	23	35	**40**	37
Lidar + MNF$_i$	23	42	**45**	38
PCA (lidar + imagery)	15	31	**44**	21
Generalized fuels types (SH, TU, and TL classes)			
Lidar alone	46	65	70	**75**
Lidar + imagery	49	69	72	**73**
Lidar + MNF$_i$	46	73	69	**76**
PCA (lidar + imagery)	50	64	66	**75**

TABLE 3. CORRELATION COEFFICIENTS OBTAINED FROM NUMEROUS ITERATIONS OF REMOTE SENSING DATA, CLASSIFICATION ALGORITHMS, AND MEASURED OR CALCULATED FUEL METRICS; THE BEST FIT BETWEEN MODEL AND DATA INPUT PER METRIC IS IN BOLD; THE TOP HALF OF THE TABLE LISTS FUEL METRICS THAT ARE USED BY ANALYSTS TO ASSIGN FUEL MODELS WHILE THOSE IN THE BOTTOM HALF OF THE TABLE ARE DIRECT INPUTS TO FIRE BEHAVIOR MODELS

			Lidar	Lidar + imagery	Lidar + MNF_i	PCA(Lidar + imagery)
Fuel model constituents	Total basal area	Linear Reg	**0.82**	**0.82**	**0.82**	0.67
		Additive Reg	0.73	0.72	0.73	0.71
		SMO	0.81	0.80	0.79	0.81
	Shrub height	Linear Reg	0.54	0.54	0.54	0.46
		Additive Reg	0.52	0.52	0.50	0.40
		SMO	0.58	0.57	0.56	**0.59**
	Shrub cover	Linear Reg	0.48	0.48	0.48	0.40
		Additive Reg	0.52	0.58	0.55	0.47
		SMO	0.59	**0.62**	0.60	0.57
	Combined fuel loads	Linear Reg	0.39	0.39	0.39	0.37
		Additive Reg	0.26	0.28	0.33	0.36
		SMO	0.40	0.43	0.43	**0.48**
	1000 hour fuel loads	Linear Reg	0.16	0.16	0.16	0.23
		Additive Reg	0.29	0.29	**0.31**	0.17
		SMO	0.27	0.27	0.27	0.18
	Fuel bed depth	Linear Reg	0.24	0.24	0.24	0.31
		Additive Reg	0.34	0.20	0.25	0.27
		SMO	0.25	0.29	0.29	**0.35**
Direct fire behavior model inputs	Canopy height (max)	Linear Reg	**0.87**	**0.87**	**0.87**	0.69
		Additive Reg	0.84	0.83	0.82	0.79
		SMO	0.86	0.85	0.85	0.82
	Canopy height (mean)	Linear Reg	**0.60**	**0.60**	**0.60**	0.44
		Additive Reg	0.55	0.54	0.53	0.54
		SMO	0.53	0.51	0.50	0.51
	Canopy cover	Linear Reg	0.62	0.62	0.62	0.74
		Additive Reg	0.72	0.72	0.73	0.76
		SMO	0.78	0.79	0.81	**0.83**
	CBH	Linear Reg	0.39	0.39	0.39	0.35
		Additive Reg	0.36	0.34	0.31	0.34
		SMO	0.32	0.33	0.34	**0.41**
	CBD	Linear Reg	0.14	0.14	0.11	0.13
		Additive Reg	0.20	0.18	**0.25**	0.19
		SMO	0.11	0.12	0.15	0.13

investigating whether radar or waveform lidar systems are more suitable in assessing FMs than a discrete, small-footprint lidar system. Radar may be more reliable because of its ability to penetrate and describe some depth of soil, although at much coarser resolution. Waveform lidar may also be beneficial because of its ability to better describe the vertical structure of the forest, and in particular, of shrub and surface level vegetation.

We should mention that in addition to the analysis and results presented here, we have also used lidar + PCA of imagery as an input, and in the FMs analysis, we used another regression tree (C4.5 J48 classifier) and an SVM (LibSVM) algorithm. These results are not presented for brevity; however, in all cases, these results produced neither best nor worst results when predicting either the FMs or the forest metrics.

	Best correlation	Method	Lidar	Lidar + imagery	Lidar + MNF$_i$	PCA(Lidar + imagery)
Canopy height (max)	0.87	L Reg	x	x	x	
Canopy cover	0.83	SMO				x
Total basal area	0.82	L Reg	x	x	x	
Shrub cover	0.62	SMO		x		
Canopy height (mean)	0.60	L Reg	x	x	x	
Shrub height	0.59	SMO				x
Combined fuel loads	0.48	SMO				x
CBH	0.41	SMO				x
Fuel bed depth	0.35	SMO				x
1,000 hour fuel loads	0.32	A Reg				
CBD	0.25	A Reg			x	

Our fuel metric results varied in accuracy. One contributing factor to the varied success rate is the relative vertical position of the measured metric within the canopy. The metrics near the top of the canopy (e.g. canopy height, $r^2=0.87$) are predicted with better accuracy than metrics near mid-canopy (e.g., shrub height, $r^2 = 0.59$), or the still worse, near-ground level metrics (e.g., fuel bed depth, $r^2 = 0.35$). Weakening laser pulse strength as it penetrates through the canopy towards the ground level and then back up, especially in dense forests, most likely plays the key role in this phenomenon. Further, in general, the fuel metric results indicate that (a) the less complex metrics (e.g., tree height) are best predicted by simple lidar data input and multiple linear regression, while (b) the more complex metrics (related to understory or fuel loads) are best predicted by the SMO support vector machine learning algorithm using PCA transform of lidar and imagery.

Our analyses of specific surface FMs, as defined by Scott and Burgan (2005), show that these are difficult to reliably predict from lidar and multispectral imagery. The CART algorithm performed best, although these results were poor and should be considered with caution. There are three main reasons for this. The first has to do with the study area: steep terrain in combination with dense, mixed-conifer vegetation, especially in comparison to previous studies of similar topics, make characterizing the forest floor problematic. Previous studies have shown that steep slopes and dense vegetation decrease the accuracy of lidar (Yu *et al.*, 2005; Hollaus *et al.*, 2006; Su and Bork, 2006; Kaartinen *et al.*, 2012). We hypothesize that the good statistical fits reported by Mutlu *et al.* (2008) between surface FMs and lidar data were in part due to a near-sea-level, flat forest study area consisting of tree plantations and old-growth pine stands. Dense vegetation may influence poor detection rates of FMs because the lidar laser pulse may not adequately penetrate the canopy structure in these situations, a critical step in accurately assessing surface fuel structure. It may be worth investigating whether a lidar-based

approach works for other terrains on less extreme slopes or sparser vegetation.

The second has to do with the physics of the lidar instrument. The FM assessment as described by Anderson (1982) and Scott and Burgan (2005) depends largely on the amount of dead fuel on the ground, fuel bed depth, and the moisture of extinction of dead fuels. The detection of these characteristics directly from airborne lidar technology is very challenging. For the most part, these are not directly measured but approximated by the surrounding environment, slope, aspect, and vegetation type.

Finally, FM assignment depends heavily on expert knowledge and is often an iterative process. The expert knowledge may include familiarity with the study area, fire behavior and FMs in the area, and potential reassignment of FMs based on preliminary fire behavior model outputs. As a result, there is not always good correspondence between FMs and the original data from which they were derived. This is further shown by the fact that lidar can predict the general fuel types but not the specific FMs. Predicting FMs using lidar in a classification context may therefore not be desirable.

We do not want to discount the potential benefits of using lidar in FM assessment. As demonstrated in this study, using lidar and/or imagery to detect general fuel model types (SH, TU, and TL) works reasonably well: up to 76 percent correct classification. The SMO algorithm consistently performed best in predicting these fuel types in comparison to statistical clustering or regression models. Further, lidar is capable of mapping some canopy metrics well (canopy cover, tree height, BA, etc), and this information, in addition to general fuel types and field data, could be used by experts to improve future FM assignment. While lidar data may not provide the perfect solution in fuel mapping, it may be the best available option and can still provide a more reliable answer than the currently accepted and mostly unreported methods used for fuel model assignment.

Conclusions

In this study, we used a range of algorithms and combinations of discrete, small-footprint lidar and multispectral imagery to predict standard surface fuel models, their constituent inputs, and fuel metrics typically used in fire behavior models such as FARSITE. We performed an extensive analysis to determine what is the optimal combination of data inputs and methods in order to predict each of the above forest metrics and/or fuel models.

Our results indicate that the specific surface fuel models are difficult to predict reliably using lidar and imagery data in a dense forest within complex terrain, regardless of the input data transformation or the methods used. However, more general fuel types were detected at a reasonable rate of 76 percent accuracy using the SMO version of SVM algorithm. The SVM predicted above 73 percent of fuel types using all data inputs. Our analyses show that deriving canopy stand structure or continuous fuel metrics is repeatable and accurate. In general, we found that to derive the less complex metrics (e.g., tree height), lidar data alone with simple multiple linear regression works best, while for the metrics that are more difficult to measure (e.g., fuel loads), best results are obtained through more sophisticated analysis with SVM using PCA transform of lidar and imagery as the input. Further, as the lidar pulse weakens when it penetrates down through the canopy, so does the pulse density and the prediction accuracy level of the associated metrics. In particular, maximum canopy height, canopy cover, and BA were described with up to 0.87, 0.83, and 0.82 Pearson's

correlation coefficient, respectively. As we move deeper into the canopy, the ability to reliably predict fuel metrics declines. The best shrub prediction was 0.62, while the prediction of ground-based fuels declined below 0.50 correlation coefficient.

Acknowledgements

References

Andersen, H.E., R.J. McGaughey, and S.E. Reutebuch, 2005. Estimating forest canopy fuel parameters using LIDAR data, *Remote Sensing of Environment*, 94(4):441–449.

Anderson, H.E., 1982. *Aids to Determining Fuel Models for Estimating Fire Behavior*, April 1982, Ogden, Utah (General Technical Report INT-122, Intermountain Forest and Range Experiment Station, Ogden, Utah), pp. 1–22.

Bertolette, D.R., and D.B. Spotskey, 1999. Fuel model and forest type mapping for FARSITE input, *Proceedings of the Joint Fire Science Conference and Workshop*, Boise, Idaho (University of Idaho and International Association of Wildland Fire), pp. 1–8.

Breiman, L., 2001. Random forests, *Machine Learning*, 45:5–32.

Brown, J.K., and P.J. Roussopoulos, 1974. Eliminating biases in planar intersect method for estimating volumes of small fuels, *Forest Science*, 20(4):350–356.

Carlton, D., 2005. *Fuel Management Analyst Plus*, version 3.0., Estacada, OR. (Fire Program Solutions, LLC., Estacada, OR.),

Chen, Q., D. Baldocchi, P. Gong, and M. Kelly, 2006. Isolating individual trees in a savanna woodland using small footprint lidar data, *Photogrammetric Engineering & Remote Sensing*, 72(8):923–932.

Collins, B., J. Miller, M. Kelly, J.W. Van Wagtendonk, and S.L. Stephens, 2008. Interactions among wildland fires in a long-established Sierra Nevada natural fire area, *Ecosystems*, 12(1):15.

Collins, B.M., R.G. Everett, and S.L. Stephens, 2011a. Impacts of fire exclusion and recent managed fire on forest structure in old growth Sierra Nevada mixed-conifer forests, *Ecosphere*, 2(4):14.

Collins, B.M., S.L. Stephens, J.J. Moghaddas, and J. Battles, 2010. Challenges and approaches in planning fuel treatments across fire-excluded forested landscapes, *Journal of Forestry*, January/February 2010:24–31.

Collins, B.M., S.L. Stephens, G.B. Roller, and J.J. Battles, 2011b. Simulating fire and forest dynamics for a landscape fuel treatment project in the Sierra Nevada, *Forest Science*, 57(2): 77–88.

Cruz, M.G., and M.E. Alexander, 2010. Assessing crown fire potential in coniferous forests of western North America: A critique of current approaches and recent simulation studies, *International Journal of Wildland Fire*, 19(4):377–398.

Duda, R., P. Hart, and D. Stork, 2001. *Pattern Classification*, John Wiley & Sons, Inc., New York, 654 p.

Feldesman, M.R., 2002. Classification trees as an alternative to linear discriminant analysis, *American Journal of Physical Anthropology*, 119:257–275.

Finney, M.A., 1998. FARSITE: Fire Area Simulator-Model Development and Evaluation, Missoula, Montana (USDA Forest Service, Research Paper RMRS-RP-4, Rocky Mountain Forest and Range Experiment Station, Missoula, Montana), pp. 1–52.

Finney, M.A., 2001. Design of regular landscape fuel treatment patterns for modifying fire growth and behavior, *Forest Science*, 47:2.

Finney, M.A., 2006. An overview of FlamMap fire modeling capabilities, *Fuels Management- How to Measure Success*, 28-30 March, Portland, Oregon (USDA Forest Service, Proceedings RMRS-P-41, Rocky Mountain Research Station, Fort Collins, Colorado), pp. 213–220.

Frank, E., M. Hall, G. Holmes, R. Kirkby, B. Pfahringer, I.H. Witten, and L. Trigg, 2010. Weka- A machine learning workbench for data mining, *Data Mining and Knowledge Discovery Handbook*, pp. 1269–1277.

Friedman, J., 2002. Stochastic gradient boosting, *Computational Statistics & Data Analysis*, 38(4):367–378.

Gatziolis, D., 2011. Dynamic range-based intensity normalization for airborne, discrete return lidar data of forest canopies, *Photogrammetric Engineering & Remote Sensing*, 77(3):251–259.

Guo, Q., W. Li, H. Yu, and O. Alvarez, 2010. Effects of topographic variability and lidar sampling density on several DEM interpolation methods, *Photogrammetric Engineering & Remote Sensing*, 76(6):701–712.

Hollaus, M., W. Wagner, C. Eberhöfer, and W. Karel, 2006. Accuracy of large-scale canopy heights derived from LiDAR data under operational constraints in a complex alpine environment, *ISPRS Journal of Photogrammetry and Remote Sensing*, 60(5):323–338.

Hsu, C.W., C.C. Chang, and C.J. Lin, 2003. A practical guide to support vector classification, Taipei, Taiwan (National Taiwan University, Taipei, Taiwan), pp. 1–16.

Hudak, A.T., N.L. Crookston, J.S. Evans, D.E. Hall, and M.J. Falkowski, 2008. Nearest neighbor imputation of species-level, plot-scale forest structure attributes from LiDAR data, *Remote Sensing of Environment*, 112(5):2232–2245.

Hyyppä, J., O. Kelle, M. Lehikoinen, and M. Inkinen, 2001. A segmentation-based method to retrieve stem volume estimates from 3-D tree height models produced by laser scanners, *IEEE Transactions on Geoscience and Remote Sensing*, 39(5):969–975.

ITT Visual Information Solutions, 2009. ENVI software, Boulder, Colorado.

Jia, G.J., I.C. Burke, A.F.H. Goetz, M.R. Kaufmann, and B.C. Kindel, 2006. Assessing spatial patterns of forest fuel using AVIRIS data, *Remote Sensing of Environment*, 102(3- 4):318–327.

Kaartinen, H., J. Hyyppa, X. Yu, M. Vastaranta, H. Hyyppa, A. Kukko, M. Holopainen, C. Heipke, M. Hirschmugl, and F. Morsdorf, 2012. An international comparison of individual tree detection and extraction using airborne laser scanning, *Remote Sensing*, 4(4):950–974.

Keane, R.E., J.L. Garner, K.M. Schmidt, D.G. Long, J.P. Menakis, and M.A. Finney, 1998. *Development of Input Data Layers for the FARSITE Fire Growth Model for the Selway- Bitterroot Wilderness Complex, USA*, Ogden, Utah (General Technical Report, Ogden, Utah), pp. 66.

Keerthi, S.S., S.K. Shevade, C. Bhattacharyya, and K.R.K. Murthy, 2001. Improvements to Platt's SMO algorithm for SVM classifier design, *Neural Computation*, 13(3):637–649.

Koch, B., U. Heyder, and H. Weinacker, 2006. Detection of individual tree crowns in airborne lidar data, *Photogrammetric Engineering & Remote Sensing*, 72(4):357–363.

Kohavi, R., 1995. A study of cross-validation and bootstrap for accuracy estimation and model selection, *International Joint Conference on Artificial Intelligence*, Stanford University, pp. 1137–1145.

Lefsky, M.A., W.B. Cohen, D.J. Harding, G.G. Parker, S.A. Acker, and S.T. Gower, 2002. Lidar remote sensing of above-ground biomass in three biomes, *Global Ecology and Biogeography*, 11(5):393–399.

Lefsky, M.A., D. Harding, W.B. Cohen, G. Parker, and H.H. Shugart, 1999. Surface lidar remote sensing of basal area and biomass in deciduous forests of eastern Maryland, USA, *Remote Sensing of Environment*, 67(1):83–98.

Lim, K., P. Treitz, M.A. Wulder, B. St-Onge, and M. Flood, 2003. LiDAR remote sensing of forest structure, *Progress in Physical Geography*, 27(1):88–106.

Lin, C., G. Thomson, C.-S. Lo, and M.-S. Yang, 2011. A multi-level morphological active contour algorithm for delineating tree crowns in mountainous forest, *Photogrammetric Engineering & Remote Sensing*, 77(3):241-249.

Miller, J.D., H.D. Safford, M. Crimmins, and A.E. Thode, 2009. Quantitative evidence for increasing forest fire severity in the Sierra Nevada and southern Cascade Mountains, California and Nevada, USA, *Ecosystems*, 12(1):16–32.

Mitchell, J.J., N.F. Glenn, T.T. Sankey, D.R. Derryberry, M.O. Anderson, and R.C. Hruska, 2011. Small-footprint lidar estimations of sagebrush canopy characteristics, *Photogrammetric Engineering & Remote Sensing*, 77(5):521–530.

Moghaddas, J.J., B.M. Collins, K. Menning, E.E.Y. Moghaddas, and S.L. Stephens, 2010. Fuel treatment effects on modeled landscape-level fire behavior in the northern Sierra Nevada, *Canadian Journal of Forest Research*, 40:14.

Mutlu, M., S.C. Popescu, C. Stripling, and T. Spencer, 2008. Mapping surface fuel models using lidar and multispectral data fusion for fire behavior, *Remote Sensing of Environment*, 112(1):274–285.

Naesset, E., and T. Gobakken, 2008. Estimation of above- and below-ground biomass across regions of the boreal forest zone using airborne laser, *Remote Sensing of Environment*, 112(6):3079–3090.

Persson, A., J. Holmgren, and U. Söderman, 2002. Detecting and measuring individual trees using an airborne laser scanner, *Photogrammetric Engineering & Remote Sensing*, 68(9):925–932.

Peterson, B., R. Dubayah, P. Hyde, M. Hofton, J.B. Blair, and J.A. Fites-Kaufman, 2005. Use of LIDAR for forest inventory and forest management application, *Proceedings of the Seventh Annual Forest Inventory and Analysis Symposium*, pp. 193–202.

Peterson, B.E., 2005. *Canopy Fuels Inventory and Mapping Using Large-footprint Lidar*, Ph.D.dissertation, University of Maryland - College Park, 218 p.

Popescu, S.C., and R.H. Wynne, 2004. Seeing the trees in the forest: Using lidar and multispectral data fusion with local filtering and variable window size for estimating tree height, *Photogrammetric Engineering & Remote Sensing*, 70(5):589–604.

Popescu, S.C., R.H. Wynne, and R.F. Nelson, 2003. Measuring individual tree crown diameter with lidar and assessing its influence on estimating forest volume and biomass, *Canadian Journal of Remote Sensing*, 29(5):564–577.

Reinhardt, E., D. Lutes, and J. Scott, 2006a. FuelCalc: A method for estimating fuel characteristics, *Fuels Management - How to Measure Success*, Fort Collins, Colorado (USDA, Forest Service, Rocky Mountain Research Station), pp. 273–282.

Reinhardt, E., J. Scott, K. Gray, and R. Keane, 2006b. Estimating canopy fuel characteristics in five conifer stands in the western United States using tree and stand measurements, *Canadian Journal of Forest Research*, 36(11):2803–2814.

Riaño, D., E. Chuvieco, J. Salas, A. Palacios-Orueta, and A. Bastarrika, 2002. Generation of fuel type maps from Landsat TM images and ancillary data in Mediterranean ecosystems, *Canadian Journal of Forest Research-Revue Canadienne De Recherche Forestiere*, 32(8):1301–1315.

Riaño, D., E. Chuvieco, S. Ustin, J. Salas, J. Rodríguez-Pérez, L. Ribeiro, D. Viegas, J. Moreno, and H. Fernández, 2007. Estimation of shrub height for fuel-type mapping combining airborne LiDAR and simultaneous color infrared ortho imaging, *International Journal of Wildland Fire*, 16(3):341–348.

Riaño, D., E. Meier, B. Allgöwer, E. Chuvieco, and S.L. Ustin, 2003. Modeling airborne laser scanning data for the spatial generation of critical forest parameters in fire behavior modeling, *Remote Sensing of Environment*, 86(2):177–186.

Rothermel, R.C., 1972. A mathematical model for predicting fire spread in wildland fuels, Ogden, Utah (USDA Forest Service, Research Paper INT-115, Intermountain Forest and Range Experiment Station, Ogden, Utah), pp. 1–40.

Saatchi, S., K. Halligan, D.G. Despain, and R.L. Crabtree, 2007. Estimation of forest fuel load from radar remote sensing, *IEEE Transactions on Geoscience and Remote Sensing*, 45(6):1726–1740.

Scott, J.H., and R.E. Burgan, 2005. *Standard Fire Behavior Fuel Models: A Comprehensive Set for Use with Rothermel's Surface Fire Spread Model, Fort Collins, Colorado* (General Technical Report, Rocky Mountain Research Station, Fort Collins, Colorado), pp. 72.

Scott, J.H., and E.D. Reinhardt, 2001. *Assessing Crown Fire Potential by Linking Models of Surface and Crown Fire Behavior*, Fort Collins, Colorado (Research Paper RMRS-RP- 29, USDA Forest Service, Rocky Mountain Research Station, Fort Collins, Colorado), pp. 59.

Skinner, C.N., and C.R. Chang, 1996. Fire *Regimes, Past and Present, Davis, California (Sierra Nevada Ecosystem Project*, Final Report to Congress: Assessments and scientific basis for management option, University of California, Centers for Water and Wildland Resources, Davis, California), pp. 1041–1069.

Skowronski, N., K. Clark, R. Nelson, J. Hom, and M. Patterson, 2007. Remotely sensed measurements of forest structure and fuel loads in the Pinelands of New Jersey, *Remote Sensing of Environment*, 108(2):123–129.

Soininen, A., 2012. *Terra Scan for MicroStation, User's Guide* (Terrasolid Ltd., Jyvaskyla, Finland).

Stephens, S.L., 2001. Fire history differences in adjacent Jeffrey pine and upper montane forests in the eastern Sierra Nevada, *International Journal of Wildland Fire*, 10(2):161–167.

Stephens, S.L., and B.M. Collins, 2004. Fire regimes of mixed conifer forests in the north-central Sierra Nevada at multiple spatial scales, *Northwest Science*, 78(1):12–23.

Stephens, S.L., R.E. Martin, and N.E. Clinton, 2007. Prehistoric fire area and emissions from California's forests, woodlands, shrublands and grasslands, *Forest Ecology and Management*, 251(3):11.

Stephens, S.L., and L. Ruth, 2005. Federal forest-fire policy in the United States, *Ecological Applications*, 15(2):532–542.

Su, J., and E. Bork, 2006. Influence of vegetation, slope and lidar sampling angle on DEM accuracy, *Photogrammetric Engineering & Remote Sensing*, 72(11):1265–1274.

Sugihara, N., J. Wagtendonk, K. Shaffer, J. Fites-Kaufman, and A. Thode, 2006. *Fire in California's Ecosystems*, University of California Press, Berkeley, California.

van Wagtendonk, J.W., 1996. *Use of a Deterministic Fire Growth Model to Test Fuel Treatments, Davis* (Sierra Nevada Ecosystem Project: Final Report to Congress: assessments and scientific basis for management option, University of California, Centers for Water and Wildland Resources, Davis, California), pp. 1155–1166.

van Wagtendonk, J.W., J.M. Benedict, and W.M. Sydoriak, 1998. Fuel bed characteristics of Sierra Nevada conifers, *Western Journal of Applied Forestry*, 13(3):73–84.

van Wagtendonk, J.W., and P.E. Moore, 2010. Fuel deposition rates of montane and subalpine conifers in the central Sierra Nevada, California, USA, *Forest Ecology and Management*, 259(10): 2122–2132.

van Wagtendonk, J.W., and R.R. Root, 2003. The use of multi-temporal Landsat Normalized Difference Vegetation Index (NDVI) data for mapping fuel models in Yosemite National Park, USA, *International Journal of Remote Sensing*, 24(8):1639–1651.

Varner, J.M., and C.R. Keyes, 2009. Fuels treatments and fire models: errors and corrections, *Fire Management Today*, 69(3):47–50.

Wulder, M.A., C.W. Bater, N.C. Coops, T. Hilker, and J.C. White, 2008. The role of LiDAR in sustainable forest management, *The Forestry Chronicle*, 84(6):807–826.

Yu, X., H. Hyyppä, H. Kaartinen, J. Hyyppä, E. Ahokas, and S. Kaasalainen, 2005. Applicability of first pulse derived digital terrain models for boreal forest studies, *Proceedings of ISPRS WG III/3, III/4 "Laser Scanning 2005,"* Enschede, the Netherlands, pp. 12–14.